Coordinated Analysis of Organic Matter in Primitive Meteorites N. Nevill[1], S. J. Clemett[2], S. Messenger[3] & K. L. Thomas-Keprta[4], [1]Curtin University of Technology, Science and Engineering division, GPO Box U1987, Perth, Western Australia, 6845, [2]ERC Inc. / [3]Robert M Walker Laboratory for Space Science, ARES, NASA Johnson Space Center, Houston, TX, USA, [4]Barrios, Engineering Science Contract Group (ESCG), 2224 Bay Area Blvd, Houston, Texas 77058, USA.

Introduction: Carbonaceous chondrites (CC) preserve a diverse range of organic matter formed within cold interstellar environments, the solar nebula, and during subsequent parent body asteroidal processing. This organic matter maintains a unique geochemical and isotopic record of organic evolution [1-4].

Bulk studies of organics within CC have revealed a complex array of organic species. However, bulk studies invariably involve solvent extraction, resulting in a loss of spatial context of the host mineral matrix [3, 5]. Correlated *in situ* chemical and isotopic studies suggest preservation of interstellar organics in the form of spherical, often hollow, micrometer sized organic nanoglobules. Nanoglobules often exhibit significant $\delta^{15}N$ and δD enrichments that imply formation through fractionation of ion-molecule reactions within cold molecular clouds and/or the outer protoplanetary disk [5]. *In situ* studies such as 6-8 are necessary to understand the organic evolutionary stages of nanoglobules and other components in the nebula and parent body [7].

We carried out coordinated *in situ* μm-scale chemical, mineralogical and isotopic studies of the Murchison (CM2), QUE 99177 (CR3), and Tagish Lake (C2 Ung) CC. These studies were performed using fluorescent microscopy, two-step laser mass spectrometry (μL^2MS), NanoSIMS, and Scanning Electron Microscopy (SEM) with Energy Dispersive X-Ray Spectroscopy (EDX). Comparative analysis of three different meteorites will help reveal the effects of parent body processes on the chemistry and isotopic composition of organic matter.

Approach and Methodology: Matrix samples ~20-40μm in size were pressed onto Au foil with an optically flat sapphire window. This provided a flat surface for chemical and isotopic imaging while still maintaining local context of surrounding matrix material. Samples were not chemically treated or embedded within a medium e.g. epoxy resin. All samples were prepared in a clean room to minimize contamination.

Optical and ultraviolet (UV) imaging was utilized for initial sample characterization and non-destructive observation of the spatial distribution of organic species containing aromatic and/or conjugated functional groups [9]. Analysis was conducted on an Olympus BX60 microscope equipped with both UV and optical imaging light sources.

The μL^2MS utilized a two-step laser method producing spectral maps, recording the molecular and spatial distribution of organic matrix matter at a ~2μm scale.

NanoSIMS C and N isotopic images were obtained with <200 nm spatial resolution using a focused 16 keV Cs^+ primary ion beam to obtain ^{12}C, ^{13}C, ^{16}O, $^{12}C^{14}N$, $^{12}C^{15}N$ & ^{28}Si images. Terrestrial kerogen was utilized as a standard for analyses.

SEM-EDX. Analysis was conducted using a JEOL 7600F field emission SEM operating at 15 keV. Samples were coated with 2 nm of Pt prior to analysis to reduced surface charging.

Results: Figures 1 & 2 show the correlation between UV imaging, a mass integrated μL^2MS spectral map (17-250 amu) and NanoSIMS ^{12}C and $\delta^{15}N$ isotopic images. Results indicate variations in organic spatial distributions at the micron scale (Fig. 1 & 2), with detection of insoluble macromolecular matter (i.e. meteoritic kerogen) through diffuse green fluorescence (λ ~ 500 nm). The prominent fluorescent hot spots (Fig. 1) and aggregate clusters of yellow fluorescent emissions (λ ~ 600 nm) were often associated with $\delta^{15}N$ hot spots (Fig. 2). QUE99177 was notable in having the most pronounced fluorescence. A similar correlation was also observed within Tagish Lake, with Murchison remaining the exception.

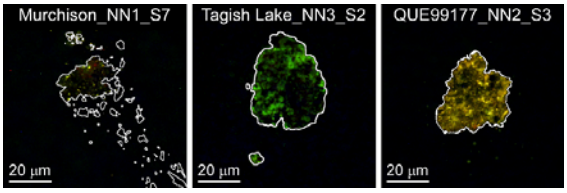

Fig 1. UV images of Murchison, QUE99177 and Tagish Lake showing diffuse green fluorescence.

During sample preparation of QUE99177 some samples did not adhere to the *Au* foil resulting in partial matrix removal, maintaining only a thin layer for further analysis. This subsequently proved fortuitous, with residual matrix showing an absence of nanoglobules, enabling a direct comparison of nanoglobule-rich and nanoglobule free matrix as illustrated in Fig. 3. The nanoglobule-enriched region was significantly enhanced in O-enriched organic species such as formaldehyde ($H_2C{=}O$) and acetaldehyde ($CH_3C{=}OH$).

Murchison and Tagish Lake showed a correlation between the abundance of O and N-rich organic species and nanoglobule abundance. Tagish lake nanoglobule enriched regions contained urea and methanethiol that

were not observed elsewhere. Murchison on average exhibited a high abundance of higher molecular weight species (> 100 amu) and H_2S compared to QUE99177 and Tagish Lake.

Figure 2 shows the spatial distribution of $\delta^{15}N$ spots across NN2_S3. Within this sample, 56 isotopically anomalous regions exceeding $\delta^{15}N$ = + 500 ‰ were identified; ranging from $\delta^{15}N$ = 500 ‰ ± 24 ‰ to $\delta^{15}N$ = 1200 ‰ ± 71‰. Figure 4 compares the $\delta^{15}N$ with the number of $^{12}C^{14}N$ counts of 500 nm-sized regions in the three meteorites. Large $\delta^{15}N$ enrichments were very common in QUE99177, less common in Tagish Lake, and rare in Murchison. Several $\delta^{15}N$-rich points in QUE999177 showed $\delta^{13}C$ anomalies of $\delta^{13}C$ = -170 ‰ ± 21 ‰ to -100 ‰ ± 24 ‰.

SEM-EDX analysis identified a correlation between the number of Nanoglobules and degree of hydrothermal parent body processing, with QUE99177 constituting an anhydrous matrix.

Discussion: Variations in spatial distribution may have resulted from geochromatography during parent body processing.

We suggest that the relationship between O-containing carbonyl species and hydrothermal alteration represents partial degradation/depolymerisation of organic nanoglobules during parent body processing, and is consistent with the formation of organic nanoglobules via carbonyl condensation reactions [10].

In situ analyses indicate chemical variations between different nanoglobules.

Both Tagish Lake and Murchison were dominated by isotopically normal matrix with rare $\delta^{15}N$ -rich inclusions [3, 11]. However, QUE99177 exhibited anomalies associated with isotopically primitive meteoritic and cometary (IDP) samples [10]. These anomalies cannot be formed within the parent body and are likely to have formed within the cold outer regions of the protosolar disk and/or the pre-solar molecular cloud [5].

Future research will look at new CC samples, refining origins for chemical and isotopic trends within nanoglobules and their relationship to parent body processing.

References: [1] Abreu N. M. and Brearley A. J. (2010) *GCA, 74,* 1146. [2] Alexander C. M. O'D., et al., (2017) *Chemie der Erde – Geochem., 77(2),* 227. [3] Sephton M. A. (2002) *Nat. Prod. Rep., 19(3),* 292. [4] Greenwood et al. (2010) *GCA, 74(5),* 1684. [5] Nakamura-Messenger et al. (2006) *Science, 314, 1439.* [6] Pearson V.K. et al. (2007) PSS 55, 1310. [7] Nakamura-Messenger K. et al. (2013) LPSC 44, #2795. [8] Clemett S. J. et al. (2014) LPSC 45, #2896. [9] Floss C. et al. (2014) *GCA, 139,* 1. [10] Kebukawa Y. et al. (2013) *ApJ, 771,* 1146. [11] Grady M. M. et al. (2002) *Met. Planet. Sci., 37,* 713.

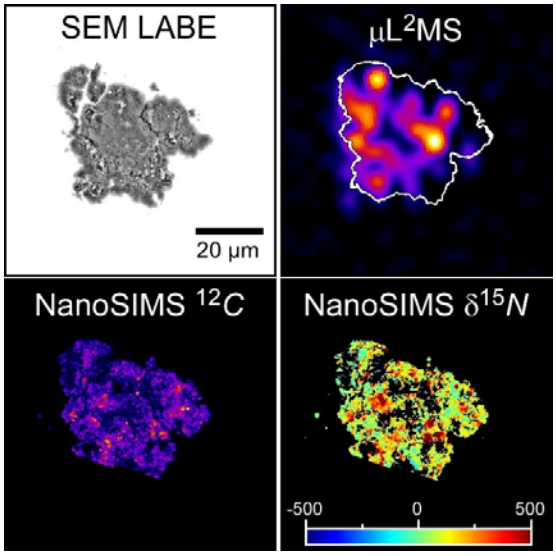

Fig 2. SEM imaging added for contextual observation of QUE99177_NN2_S3. µL²MS image map showing spatial distribution with comparative NanoSIMS elemental C map with a $\delta^{15}N$ map.

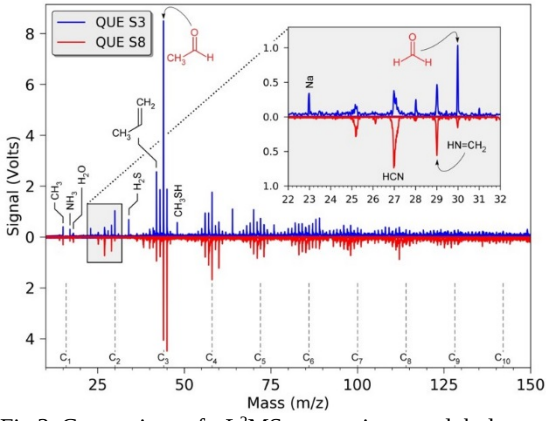

Fig 3. Comparison of µL²MS spectra in nanoglobule-rich (NN2_S3) and nanoglobule-poor (NN2_S8) matrix. The zoomed region shows O-rich speciation in NN2_S8.

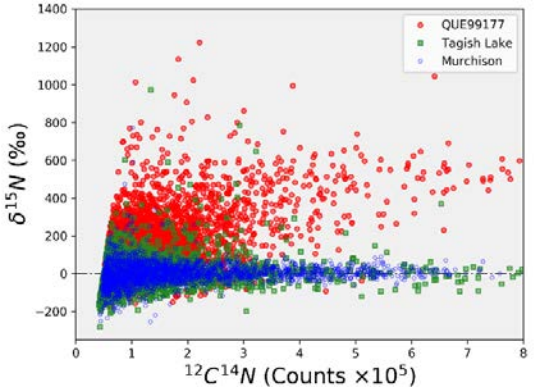

Fig 4. Bin data of isotopic anomalies identified within nitrogen rich regions across sampled matrix areas for each meteorite. All values have errors $\delta^{15}N$ < 75 ‰.